Proceedings of the 20th International Conference on Soil Mechanics and Geotechnical Engineering– Rahman and Jaksa (Eds)

Effects of particle shape and orientation on anisotropy of granular materials observed in elastic wave velocities

Effets de la forme et de l'orientation des particules sur l'anisotropie des matériaux granulaires observés à travers les vitesses de propagation des ondes élastiques

Junming Liu, Masahide Otsubo & Reiko Kuwano
Institute of Industrial Science (IIS), The University of Tokyo, 4-6-1 Komaba, Meguro-ku, Tokyo 153-8505, Japan, j-liu@iis.u-tokyo.ac.jp

Yuichiro Kawaguchi
Obayashi Corporation, Shinagawa Intercity Tower B, 2-15-2, Konan, Minato-ku, Tokyo 108-8502, Japan

ABSTRACT: Natural granular soils comprised of non-cohesive particles display directional diversity in stiffness at small strains due to the geometry of soil particles and soil packing . However, the underlying mechanism of the inherent anisotropy has not been fully unraveled partially because of the limitation in measuring multi-directional stiffness of a soil specimen accurately in the laboratory. This study focuses on the influence of particle shape and orientation after deposition on the anisotropic behaviors of granular materials. Shear wave (S-wave) velocities of four kinds of granular materials: glass beads, Toyoura sand, basmati rice and wild rice are measured by a newly developed cubical soil box equipped with planar piezoelectric transducers. The experimental results show that more elongated particle shapes contribute to larger inherent anisotropy of granular materials. And relationships among particle orientation, directions of S-wave propagation and oscillation are observed in this study. Specifically, S-waves propagating along the particle orientation are faster than those oscillating along the particle orientation. Among all the six components of S-waves in the principal directions, those neither propagating nor oscillating along the particle orientation are the slowest.

RÉSUMÉ : Les sols granulaires naturels composés de particules non cohésives présentent une anisotropie de rigidité due à l'anisotropie induite par le réseau de contacts entre les particules du sol. Cependant, les mécanismes sous-jacents de l'anisotropie induite n'ont pas été entièrement élucidés, en partie en raison de la technique limitée de mesure précise de la rigidité multidirectionnelle d'un échantillon de sol en laboratoire. Cette étude se concentre sur l'influence de la forme et de l'orientation des particules sur l'anisotropie des matériaux granulaires. Les signaux d'ondes élastiques de quatre types de matériaux granulaires (billes de verre, sable de Toyoura, riz basmati et riz sauvage) sont mesurés par un nouveau procédé consistant en une boîte cubique équipée de capteurs piézoélectriques. Les résultats expérimentaux montrent que des particules plus allongées contribuent à une anisotropie induite plus importante du matériau granulaire. De plus, cette étude se concentre sur les relations entre l'orientation des particules et les directions de propagation et d'oscillation de l'onde de cisaillement (onde S). Plus précisément, les ondes S se propageant selon l'orientation des particules progressent plus rapidement que celles dont les oscillations sont orientées selon des particules. Parmi les six composantes des ondes S dans les directions principales, celles qui ne se propagent ni n'oscillent selon l'orientation des particules sont les plus lentes.

KEYWORDS: Stiffness anisotropy; particle shape and orientation; shear wave measurement; granular material.

1 INTRODUCTION.

Natural granular soils, e.g. gravel and sand, display directional diversity in stiffness at small strains, which is called the stiffness anisotropy and is essential for geotechnical engineering design. The stiffness anisotropy in general can be classified into stress-induced anisotropy due to anisotropic stress states, and fabric-induced or inherent anisotropy caused by the soil particle characteristics and soil packing (Oda & Nakayama 1988; Wang & Mok 2008). In the past decades, many researchers have experimentally and numerically investigated the influence of inherent anisotropy on the behavior of sand (e.g. Arthur & Menzies 1972; Anandarajah & Kuganenthira 1995; Gu et al. 2017; Otsubo et al. 2020). However, the underlying mechanisms of the inherent anisotropy have not been thoroughly discussed.

The shear (S-) wave velocity (V_s) is a fundamental soil mechanical property that can reflect the inherent anisotropy. V_s can be conveniently measured by S-wave propagation tests in both field and laboratory under real and controlled conditions (Hussien & Karray 2015). Nevertheless, accurate measurement of multi-directional V_s of granular soils is still challenging for researchers. Recently, planar transducers made of piezoelectric materials have been used in research (Suwal & Kuwano 2013; Dutta et al. 2020) to measure V_s and compression (P-) wave velocity V_p in soil specimens. The planar transducer has several advantages over traditional bender elements in dynamic soil tests, by which soil specimens will not be disturbed during specimen preparation, materials with coarse particles can be measured, and more planar P- and S-waves can be generated in one test.

This study mainly focuses on the inherent anisotropy of granular materials and discusses the influence of particle shape and orientation after deposition process on the V_s anisotropy of granular materials at small strains. A cubical soil box equipped with multi-directional transducers was developed to conduct S-wave propagation tests on several granular materials, by which both P- and S-waves can be generated and received.

2 LABORATORY EXPERIMENTAL PROCEDURE

2.1 *Tested material*

Four granular materials: glass bead (GS), Toyoura sand (TS), basmati rice (BR) and wild rice (WR), were tested in this study (Fig. 1), and their physical properties are listed in Table 1.

To characterize particle shapes, the aspect ratio (*AR = minor axis / major axis*) was adopted in this study, where representative

values of *AR* were 0.933, 0.592, 0.221, 0.166 for GB, TS, BR and WR materials, respectively. These four materials were used to evaluate the influence of particle shape. And only WR specimens were used to study the influence of particle orientation due to its elongated geometry, which makes it convenient to align the WR particles in a specific direction.

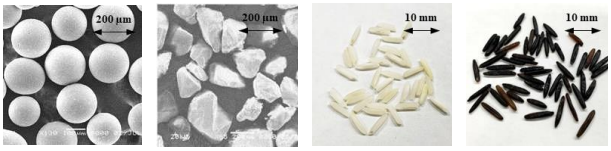

(a) (b) (c) (d)

Figure 1. Tested granular materials: (a) glass beads, (b) Toyoura sand, (c) basmati rice and (d) wild rice.

Table 1. Physical properties of the tested materials.

Material	GB	TS	BR	WR
Mean particle size (D_{50}) / mm	0.20	0.24	7.10 (major axis)	11.27 (major axis)
Specific gravity (G_s)	2.50	2.64	1.47	1.47
Max. void ratio (e_{max})	1.61	1.63	0.92	0.87
Min. void ratio (e_{min})	0.55	0.62	0.60	0.69
Aspect ratio (AR)	0.933	0.592	0.221	0.166

2.2 *Cubical soil box and shear plate configuration*

A cubical box (Fig. 2) made of acrylic plates was developed, in which a specimen with dimensions of 100×100×100mm can be prepared. The top face of the box can be adjusted to the specimen height. Three pairs of planar (square-shaped) transmitters and receivers are installed at the center of the three sets of opposite faces of the box, and each of the transmitter consists of both compression (P-) and shear (S-) type piezoelectric transducers (Fig. 3) that generate P- and S-wave, respectively.

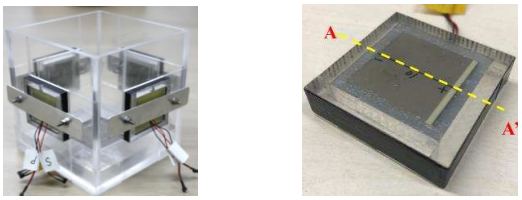

(a) (b)

Figure 2. (a) Cubical soil box and (b) planar transducer.

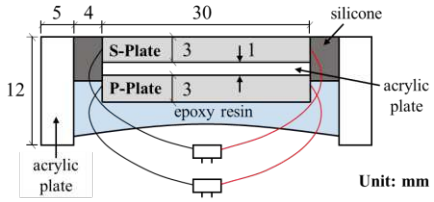

Figure 3. Design configuration of the planar transducer (A-A').

2.3 *Specimen preparation*

Specimen details are summarized in Table 2. For the evaluation of the particle shape effects, GB, TS, BR and WR were air-pluviated into the soil box in a dry condition and compacted vertically using a wooden rammer layer by layer. The 100mm height specimen was divided into ten layers, and each layer was approximately 10mm. For the tests related to the particle orientation effects, another three WR specimens were prepared in two different orientation conditions: one was the X axis orientation specimen, where the WR particles were carefully placed into the soil box and compacted vertically to make most of their major axes parallel to the X axis layer by layer, so as the other two Y axis orientation specimens (Fig. 4). S-wave propagation tests were conducted at σ'_V = 2kPa, where the stress was applied with mass on the top face of the soil box (including the weight of the top face). However, for BR specimen, test result at σ'_V = 1kPa was used due to the poor recorded signals at σ'_V = 2kPa. The relative densities of all the specimens exceed 60% (Table 1), which can be generally considered as dense state.

Table 2. Details of tested specimens.

No.	Material	Orientation	Dry density / g/cm³	Void ratio	Relative density (%)
1	GB		1.61	0.55	92
2	TS	random	1.63	0.62	87
3	BR		0.92	0.60	78
4		random	0.87	0.69	77
5	WR	X axis	0.90	0.63	94
6		Y axis	0.88	0.67	83
7		Y axis	0.89	0.65	88

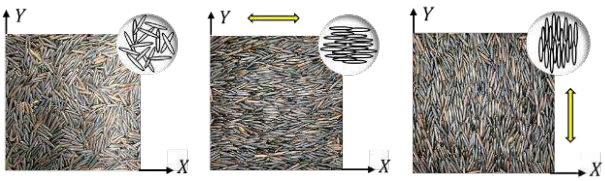

(a) (b) (c)

Figure 4. Particle orientation of specimens (top view): (a) random in XY plane (b) dominated in X axis direction (c) dominated in Y axis direction.

2.4 *Dynamic wave propagation tests*

A single period of sinusoidal pulse was used to generate S-waves at the transmitter, and the signals were recorded by the receiver at the opposite face of the soil box. The double amplitude of input excitation voltage was 140V and the input frequency was varied so that the responses of the transmitter and receiver contain similar frequency contents. The input frequency f_{in} = 7kHz was selected for GB and TS specimens and f_{in} = 3kHz was chosen for BR and WR specimens. The peak-to-peak method was adopted to determine the travel time of S-waves by calculating the time difference between the first major peaks of input and output signals (recommended by Yamashita et al. 1999).

Considering both P- and S-waves, there are nine types of elastic wave components (Fig. 5a), but the soil box used in the present study can only generate all the three types of P-waves P_{XX}, P_{YY} and P_{ZZ}, and three types of S-waves, e.g. S_{YX}, S_{XZ} and S_{ZY} (Fig. 5b) in one experiment. The first and the second subscripts indicate the S-wave propagation and oscillation directions, respectively. This study only focuses on S-waves to discuss the inherent anisotropy of the tested granular materials.

3 EXPERIMENTAL RESULTS

3.1 *Influence of particle shape*

The test results are shown in Table 3 and Fig. 6. For the tested

materials, the velocity ratios of $V_{s,HH}/V_{s,VH}$ and $V_{s,HV}/V_{s,VH}$ are compared in terms of their aspect ratios (AR). Recalling that the horizontal stress was not measured in this study, and the stress may vary with particle shape, comparison on $V_{s,HH}/V_{s,VH}$ was limited in a qualitative manner; however, the influence of particle shape on the variation of $V_{s,HH}/V_{s,VH}$ under K_0 stress states can still be assessed. Fig. 7 summarizes the velocity ratios with best-fit lines, where a decreasing trend of $V_{s,HH}/V_{s,VH}$ is observed as AR increases. The maximum value of $V_{s,HH}/V_{s,VH}$ is 1.38 for WR specimen in this study. For Toyoura sand specimen, $V_{s,HH}>V_{s,VH}$, confirming the typical trend of in-situ measurements for soils (Clayton 2011). It is only spherical GB specimen that gives $V_{s,HH}<V_{s,VH}$, which probably results from the larger stress level in the vertical direction and insignificant inherent anisotropy of the specimen composed of spherical particles. Generally, granular materials deposited vertically are supposed to exhibit cross-anisotropic deformation behaviors, which are symmetric about the vertical axis (Hoque & Tatsuoka 1997) and can be verified by the equivalence between the symmetric components of $V_{s,HV}$ and $V_{s,VH}$. In this study, regardless of the particle shape, all the tested materials show $V_{s,HV}/V_{s,VH}\approx 1$, which confirms the cross-anisotropic assumption of granular materials.

Since the discussion is based on the ratio of V_s measured from the same material, other particle characteristics that may influence the inherent anisotropy of granular materials, e.g. particle surface roughness, are insignificant to the results when the particle shape is the major variable.

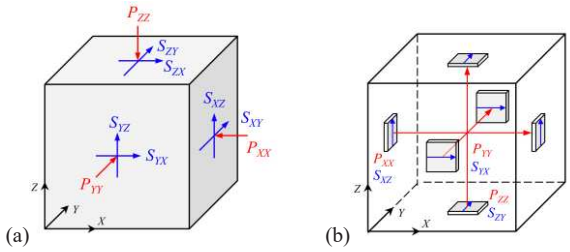

Figure 5. (a) Notation of P- and S-wave components and (b) six-types of elastic waves measured in one specimen.

Table 3. Laboratory test results of the influence of particle shape.

Material	GB	TS	BR*	WR
$V_{s,HH}/V_{s,VH}$	0.90	1.13	1.23	1.38
$V_{s,HV}/V_{s,VH}$	1.01	1.04	1.00	1.00

BR* at σ'_V = 1kPa; the others at σ'_V = 2kPa.

3.2 *Influence of particle orientation*

Three WR specimens with most of their major axes of particles aligning along either X or Y axis were prepared. They were tested under the same condition with a minor difference in void ratio to reveal the influence of particle orientation after deposition and check the repeatability of test results.

For the X axis orientation case, the sequence of $V_{s,XY}>V_{s,YX}>V_{s,ZY}$ (Table 4) indicates that S-waves traveled the fastest within the depositional plane (XY plane) when it propagated along the particle orientation, i.e. $V_{s,XY}$. It slowed down when oscillated along the particle orientation, i.e. $V_{s,YX}$. S-waves neither propagating nor oscillating along the particle orientation traveled the slowest, i.e. $V_{s,ZY}$. The results are consistent with Santamarina and Cho (2004) who conducted S-wave propagation tests on mica flacks and rice grains whose preferential particle alignment was confirmed during sample preparation.

For the Y axis orientation case, due to the limitation of the soil box used in the present study, only three types of S-waves can be measured in one experiment. Thus, two WR specimens with Y axis particle orientation were prepared to observe more types of S-waves with different combinations of propagation and oscillation directions. The sequence of $V_{s,YX}>V_{s,XY}>V_{s,ZY}>V_{s,XZ}$ (Table 4) verifies that when the particle orientation of WR dominates in one direction, the direction of S-wave propagation has stronger influence on the V_s compared with the direction of S-wave oscillation. If S-waves neither propagate nor oscillate along the particle orientation (travels within the plane perpendicular to the particle orientation), the corresponding velocities are supposed to be the lowest.

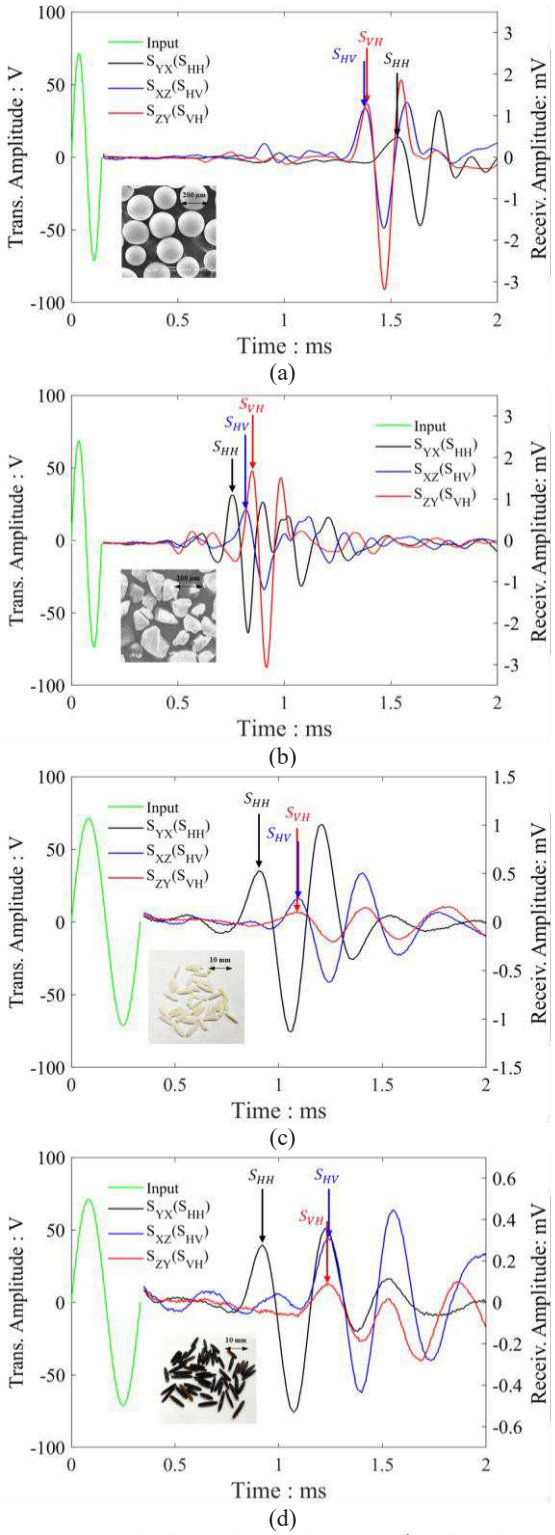

Figure 6. S-wave signals (a) glass bead (GB) at σ'_V = 2kPa, (b) Toyoura sand (TS) at σ'_V = 2kPa, (c) Basmati rice (BR) at σ'_V = 1kPa and (d) wild rice (WR) at σ'_V =2kPa.

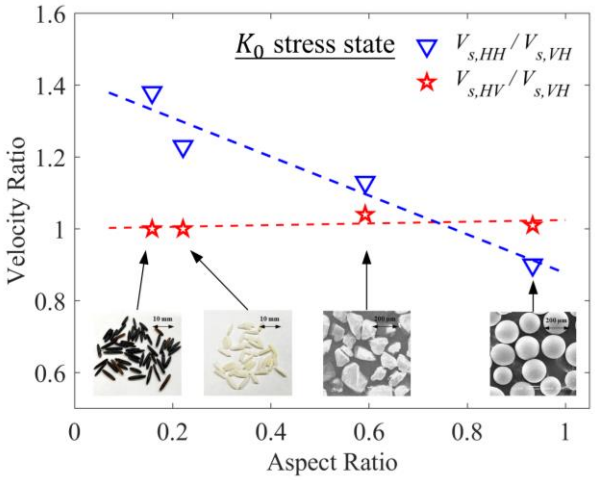

Figure 7. Sensitivity of V_s ratios with varying AR.

Table 4. Laboratory test results of the influence of particle orientation.

Orientation	$V_{s,XY}$ m/s	$V_{s,YX}$ m/s	$V_{s,YZ}$ m/s	$V_{s,ZY}$ m/s	$V_{s,XZ}$ m/s	$V_{s,ZX}$ m/s
X axis	126	118	—	80	—	—
Y axis (1)	—	116	—	110	82	—
Y axis (2)	113	124	—	101	—	—

The three specimens prepared by the same method show similar trend of the relative magnitude of V_s, confirming the repeatability of the experiments.

Three symbols of O, H and D are used to represent the three orthogonal directions: particle orientation, the direction perpendicular to particle orientation within horizontal plane and the deposition direction, respectively. According to the results above, the relative magnitude of V_s is assumed to be (the example of Y axis orientation is shown in Fig. 8):

$$V_{s,OH} > V_{s,OD} > V_{s,HO} > V_{s,DO} > V_{s,HD} > V_{s,DH} \quad (1)$$

where the first and the second subscripts indicate the direction of the S-wave propagation and oscillation, respectively, i.e. $V_{s,OH}$ represents the velocity of S-wave that propagates along particle orientation and oscillates within the horizontal plane; $V_{s,HD}$ means the velocity of S-wave that propagates perpendicularly to the particle orientation within the horizontal plane and oscillates along the deposition direction.

In general, when the particle orientation is aligned in the same direction, V_s is higher when the direction of wave propagation is parallel to the particle orientation, as compared to velocities of S-waves oscillating along the particle orientation. Among all the six components of S-waves, those neither propagating nor oscillating along the particle orientation are the slowest.

4 CONCLUSIONS

This research has assessed the influence of particle shape and orientation after deposition on the anisotropy of shear wave velocity (V_s) of granular assemblies. Multi-directional V_s were measured in the principal axis directions using a cubical soil box equipped with planar piezoelectric transducers. The experimental results are limited to relatively dense specimens under a specific specimen preparation method; however, the following conclusions can be drawn:

- V_s is influenced by the particle shape when dry pluviation method with compaction is used. For lower value of aspect ratio, i.e. more elongated particle shape, the ratio of $V_{s,HH}/V_{s,VH}$ becomes larger.
- Particle orientation has obvious influence on stiffness anisotropy of grain assemblies, which can be captured by multidirectional V_s.
- S-waves travel faster when the direction of wave propagation is parallel to the particle orientation, as compared to velocities of S-waves oscillating along the particle orientation. Among all the six components of S-waves in the principal axes, those neither propagating nor oscillating along the particle orientation are the slowest.

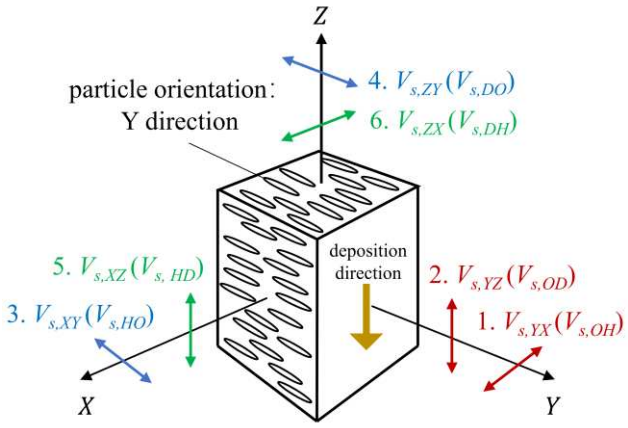

Figure 8. Relative magnitude of V_s under the influence of particle orientation (example of Y axis orientation).

5 ACKNOWLEDGEMENTS

This work was supported by JSPS KAKENHI Grant Number 19K15084.

6 REFERENCES

Anandarajah A. and Kuganenthira N. 1995. Some aspects of fabric anisotropy of soil. *Géotechnique* 45 (1), 69-81.

Arthur J.R.F. and Menzies B. 1972. Inherent anisotropy in a sand. *Géotechnique* 22 (1), 115-128.

Clayton C.R.I. 2011. Stiffness at small strain: research and practice. *Géotechnique* 61 (1), 5-37.

Dutta T.T., Otsubo M., Kuwano R. and Sato T. 2020. Estimating multidirectional stiffness of soils using planar piezoelectric transducers in a large triaxial apparatus. *Soils and Foundations* 60 (5), 1269-1286.

Gu X., Hu J. and Huang M. 2017. Anisotropy of elasticity and fabric of granular soils. *Granular Matter* 19 (2), 33.

Hoque E. and Tatsuoka F. 1998. Anisotropy in elastic deformation of granular materials. *Soils and foundations* 38 (1), 163-179.

Hussien M.N. and Karray M. 2015. Shear wave velocity as a geotechnical parameter: an overview. *Canadian Geotechnical Journal* 53 (2), 252-272.

Oda M. and Nakayama H. 1988. Introduction of inherent anisotropy of soils in the yield function. *Studies in Applied Mechanics* 20, 81-90.

Otsubo M., Liu J., Kawaguchi Y., Dutta T.T. and Kuwano R. 2020. Anisotropy of elastic wave velocity influenced by particle shape and fabric anisotropy under K_0 condition. *Computers and Geotechnics* 128, 103775.

Santamarina J.C. and Cho G.C. 2004. Soil behaviour: The role of particle shape. *Advances in geotechnical engineering: The Skempton conference: Proceedings of a three-day conference on advances in geotechnical engineering*, London, UK, 604-617.

Suwal L.P. and Kuwano R. 2013. Disk shaped piezo-ceramic transducer

for P and S wave measurement in a laboratory soil specimen. *Soils and Foundations* 53 (4), 510-524.
Wang Y.H. and Mok C.M. 2008. Mechanisms of small-strain shear-modulus anisotropy in soils. *Journal of geotechnical and geoenvironmental engineering* 134 (10), 1516-1530.